Masses of Short-Lived Nuclides: Precision Measurement Techniques and Applications

Similar to fingerprints, atoms can be identified by their masses—when weighted with sufficient accuracy. The mass of an atom reflects all internal forces and thus carries information on the strong, weak, and electromagnetic interactions both of the nucleons and the electrons. Thus, atomic masses are addressed in numerous applications, at different levels of accuracies. For atomic-physics applications, like QED tests or electron binding energies, relative mass uncertainties down to the current limit of about $\triangle m/m \approx 10^{-11}$ can be essential. In contrast, nuclear binding energies are on the MeV scale and $\triangle m/m = 10^{-6}$ to 10^{-8} is sufficient for, for example, astrophysics or tests of nuclear models (Table 1).

The method of choice to reach a mass precision of 10^{-8} and better on specific long-lived radio-nuclides is Penning trap mass spectrometry. For mass mapping of the nuclear chart and for nuclides having shorter half-lives, storage-ring mass spectrometry is a complementary approach [1]. Both methods use frequency measurements for the mass determination. The resolving power and accuracy rely on a sufficiently long measurement time and thus ion storage is an essential ingredient. In the following, both techniques and selected applications in nuclear physics will be highlighted. Other approaches of mass spectrometry on short-lived nuclides are found in recent reviews [2,3].

Production and Separation of Nuclides Far from Stability

A prerequisite for any mass measurements of exotic nuclides is their production and separation. A variety of nuclear reactions is used to produce radioactive nuclei: fission, target spallation, projectile fragmentation, fusion, deep inelastic, and nuclear transfer reactions [4]. All these reactions produce a wide variety of nuclei. Therefore, it is necessary to separate the nuclides of interest from the unwanted contaminants. Two main complementary separation techniques were developed, namely Isotope Separation On-Line (ISOL) and in-flight separation. In the former method, the exotic nuclei are produced and stopped in thick targets (up to a few 100 g/cm^2). Extraction processes are chemistry dependent and can take seconds, which, on one hand, restricts the nuclei that can be investigated [5]. On the other hand, the ISOL beams are superior in terms of intensity and optical quality and ideally suited for Penning-trap spectrometers.

In the in-flight method, the primary beams impinge on a thin target. Thus, the reaction products emerge with high kinetic energies, mainly in the forward direction. The fragments are highly ionized, which allows an efficient electromagnetic separation "in-flight." As the separation depends mainly on kinematical properties, all nuclides can be provided without any chemical restriction. The disadvantage of the inevitable phase-space enlargement of the separated beams can be compensated by coupling to storage-cooler rings.

In order to combine the best of both methods, a hybrid technique has been developed, whereby the fragments separated in-flight are thermalized in a gas cell. After fast and efficient extraction from the gas cell the rare-isotope beams of ISOL-quality are post-accelerated.

Due to their small production cross-sections and short lifetimes the nuclei far away from the valley of β-stability are difficult to investigate. Therefore, very efficient and fast experimental techniques had to be developed. Beams of separated extremely unstable nuclei are already available for precision mass spectrometry at: ISOLDE at CERN in Geneva, Switzerland, SHIP at GSI in Darmstadt, Germany, the IGISOL facility in Jyväskylä, Finland, the NSCL facility at Michigan State University, Argonne, USA, as well as at TRIUMF in Vancouver, Canada.

Penning-Trap Mass Spectrometry

A strong magnetic field confines the ions radially in the Penning trap with the Lorentz force leading to circular orbits with the mass-characteristic cyclotron frequency of revolution

$$f_c = \frac{1}{2\pi} \cdot \frac{qB}{m} \qquad (1)$$

For an ion with charge q and mass m in a magnetic field B along the direction of the magnetic field lines, that is, in the axial direction, harmonic confinement is obtained by an additional weak static electric quadrupole potential. In addition, this combination of electric and magnetic fields leads to a low-frequency circular drift motion centered in the trap axis (Figure 1, right). Thus, the trajectory of a stored ion consists of three independent harmonic modes with the corresponding magnetron (f_-), modified cyclotron (f_+) and axial frequency (f_z) [6]. The

Table 1. Fields of applications and respective required relative uncertainty of the measured mass $\delta m/m$ as well as absolute uncertainty δm (in keV) for a nuclide of mass $A = 100$.

Field of application	Research area addressed	$\delta m/m$	δm (keV)
Chemistry	Identification of molecules	10^{-4}–10^{-7}	10 keV–10 MeV
Nuclear Physics	Nuclear structure, mass models	10^{-6}–10^{-7}	10–100 keV
Astrophysics	Stellar nucleosynthesis processes	10^{-6}–10^{-7}	10–100 keV
Weak Interaction	CVC hypothesis, CKM unitarity	$\leq 10^{-8}$	≤1 keV
Metrology	Fundamental constants	$\leq 10^{-9}$	≤100 eV
Atomic Physics	Binding energies, QED	$\leq 10^{-10}$	≤10 eV
Particle Physics	CPT invariance test	$\leq 10^{-11}$	≤1 eV

sum $f_- + f_+ = f_c$, is equal to the cyclotron frequency in free space, that is, in the absence of an electric field. This "true" cyclotron frequency can be determined by applying radiofrequency signals at frequencies f_{HF} close to f_c and subsequently ejecting the ions into a drift region. In this "time-of-flight ion cyclotron resonance" (ToF-ICR) method a resonant excitation of the ion motion results in a reduced ToF to an ion detector. The frequency is scanned and the center of the ToF resonance determines f_c and thus the mass of the ion of interest. Masses of radionuclides with production rates of only 100 ions per second and half-lives as short as 10 ms have been measured with an uncertainty as low as 10^{-8}.

Storage Ring Mass Spectrometry

In contrast to several Penning trap facilities [7], there is only one storage ring that is presently pursuing high-precision mass measurements, namely the experimental storage ring ESR at GSI Darmstadt [8]. The nuclides of interest come as highly charged ions (bare, H-, and He-like) from the in-flight Fragment Separator (FRS) [9] and are injected as a 500-ns bunch into the ESR [10]. The frequencies f of the circulating ions ($f \approx 2$ MHz) can be related in first-order approximation to their mass-to-charge ratios (m/q) by the following expression [11]:

$$\frac{\Delta f}{f} = -\alpha_p \frac{\Delta(m/q)}{m/q} + \frac{\Delta v}{v}(1-\gamma^2\alpha_p), \quad (2)$$

where γ is the relativistic Lorentz factor and $\alpha_p \frac{\Delta C/C}{\Delta(B\rho)/B\rho}$ is the so-called momentum compaction factor, which characterizes the relative variation of the orbital length C per relative variation of the magnetic rigidity $B\rho$. Obviously, an unambiguous relation between f and m/q is obtained when the velocity-dependent term disappears. There are two complementary ways to achieve this (Figure 2):

1. In Schottky-Mass-Spectrometry (SMS) [12] $\Delta v/v \rightarrow 0$ is reached by the electron cooling and f is measured by Fourier analysis of the image charges induced on two pick-up electrodes by the circulating ions. Relative mass uncertainties below 10^{-7} [13] can be reached, however, due to the time needed for the electron-cooling, only for nuclides with half-lives exceeding a few seconds.
2. For Isochronous-Mass-Spectrometry (IMS) [14] the storage ring is operated at $\gamma^2 = 1/\alpha_p$, that is, the ion frequencies are independent of their velocity spread. IMS gives access to nuclides with half-lives even down to microseconds at relative uncertainties in the order of 10^{-6}. Ion detection is achieved via secondary electrons that are produced at each passage of the circulating ion through a foil mounted inside the ring aperture. The ions typically run for a few hundred revolutions.

Both methods, SMS and IMS, are extremely efficient. $\Delta(m/q)/(m/q)$ of 2.5% and 13%, respectively, can be covered simultaneously in one ion-optical setting. Moreover, the mass can be determined from a single ion. These techniques are therefore ideally suited to map large areas on the chart of nuclides.

Applications of Nuclear Masses and Mass Spectrometry

Isomer Resolution

Many nuclides have long-lived isomeric states—often with unknown

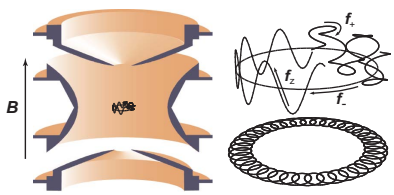

Figure 1. *Left: Sketch of a Penning trap (diameter about 2 cm). Right, top: Trajectory of charged particles inside the trap with typical amplitudes of 1 mm: Superposition of the three independent motional modes. Right, bottom: Projection onto the radial plane.*

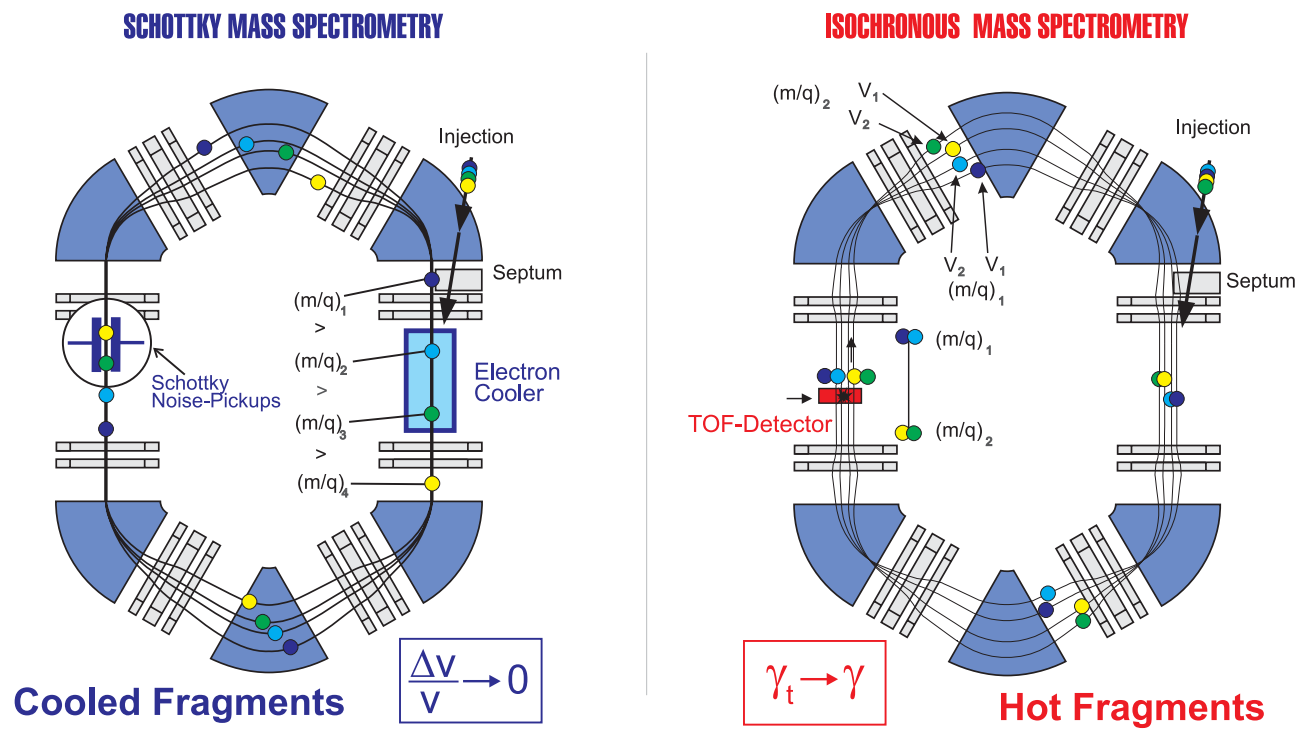

Figure 2. *Schematic illustrations of the storage ring mass spectrometry. Left: Schottky Mass Spectrometry (SMS); Right: Isochronous Mass Spectrometry (IMS) at the ESR [15].*

excitation energies. If unresolved the measurement leads to deviations from the correct ground-state mass values. To avoid such errors resolving powers $R=m/\triangle m=10^6$ and above are required. On the other hand, high-resolution mass spectrometry allows to determine isomeric-state sequences, to prepare isomerically pure beams [16], and even to discover nuclear isomers, for example, ^{65}Fe at LEBIT [17] (left part of Figure 3). $R\approx10^6$ corresponds to, for example, an excitation time of $T_{RF}\approx1$ s at $f\approx1$ MHz, that is, $B\approx7$ T for singly charged ions of mass $A\approx100$ in a Penning trap. If the half-lives allow, even higher resolving powers can be reached by further increasing T_{RF}. Alternatively, because ν_c scales with q, R can be improved considerably by increasing the charge state, as planned for TITAN at TRIUMF/Vancouver [18].

Another way to resolve isomeric and ground states is based on the fact that a single stored ion can only be present in one or another state. This is often used in SMS. Isomers with very small excitation energies can be resolved, for example, a new isomeric energy of only 103(12) keV was discovered [19] (right part of Figure 3).

Proton-Neutron Interactions and the New Masses

The mass $M(N,Z)$ of a nucleus with N neutrons and Z protons is one of the most fundamental characteristics because the binding energy $B(N,Z)=\{NM_n+ZM_p-M(N,Z)\}c^2$ (with neutron mass M_n and proton mass M_p) contains the summed effects of all nucleonic interactions. Thus the growth in number and accuracy of nuclear mass values contributes again and again to our understanding of nuclear structure. In particular masses of very neutron-rich nuclei can reveal new nuclear properties due to the strong asymmetry of their proton-to-neutron ratio. The storage-ring mass spectrometry has proven most powerful, providing in a single experiment several hundreds of mass values [12]. This gives an overview of the hills and valleys that form the mass surface $M(N,Z)$ and allows to study the influence of certain nuclear configurations and interactions.

Various correlations between nucleons can be extracted from mass differences of neighboring nuclei. For instance, a systematic study of the well-known like-nucleon pairing correlations has been performed [20]. Another class of interactions is that of

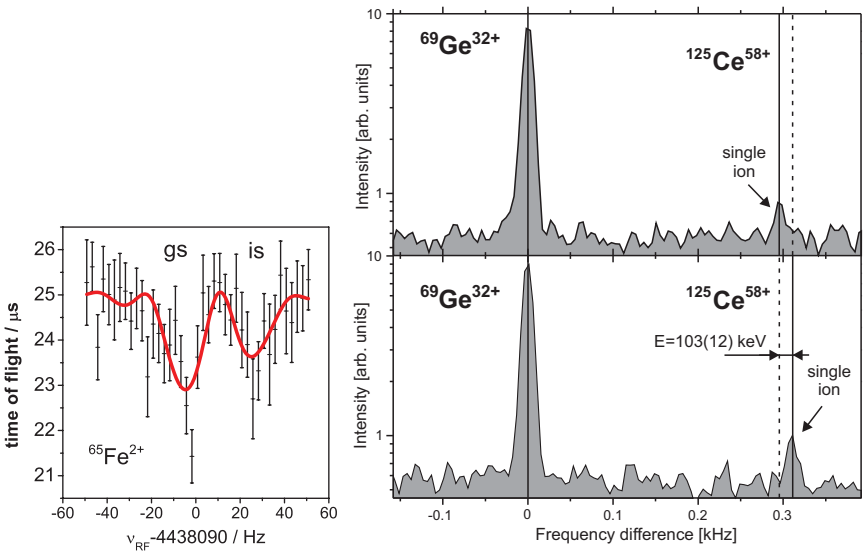

Figure 3. *Left: Time-of-flight cyclotron resonance of $^{65}Fe^{2+}$ (ground state "gs" and isomeric state "is") using an excitation time of 50 ms. A fit of the theoretical line shape to the data is added [17]. Right: Schottky frequency spectra of single stored $^{125}Ce^{58+}$ ions in the ground and isomeric states. This isomer was not known before Ref. [19]. The peaks of $^{69}Ge^{32+}$ ions are shown as a reference.*

the last proton(s) with the last neutron(s), defined by

$$\delta V_{pn}(Z,N) = \tfrac{1}{4}[\{B(Z,N) - B(Z,N\text{-}2)\} - \{B(Z\text{-}2,N) - B(Z\text{-}2,N\text{-}2)\}]$$

for even-even nuclei. For example, δV_{pn} values show striking singularities for nuclei with $N=Z$, reflecting the $T=0$ interaction. Recently, δV_{pn} values from masses of the latest Atomic Mass Evaluation AME2003 [21] highlighted the variations of the *p-n* interaction [22,23]. δV_{pn} values describe and explain the shell structure and orbit occupations near the Fermi surface, for example in the rare-earth region (see Figure 4). Because δV_{pn} varies by about 150–250 keV in a given region, its uncertainties should be below 30–50 keV. Because four masses enter in the $\delta V_{pn}(Z,N)$ equation, trends can be distinguished unambiguously only if the uncertainties of the individual mass values are of the order of 10–20 keV, that is, $\delta m/m < 1\times10^{-7}$ for nuclides above $A \approx 100$.

Testing of New Mass Models by Nuclear Masses Far from Stability

Due to the lack of an exact description of the strong interaction and the complexity of the many-body nucleonic system, the nuclear binding energy is not readily predicted by *ab initio* theories. Instead, one has to rely on phenomenological (macroscopic-microscopic) mass models or mass formulas aiming at a quantitative prediction of atomic masses [2]. They make use of a set of free parameters (up to several hundreds), which have to be constrained by fitting to experimental data. In particular data far from the valley of β-stability can act as test cases for the predictive power of the models and formulas, as demonstrated in Figure 5.

In the last few years there has been significant progress in the construction of microscopic mass models on the basis of self-consistent mean-field models. Large-scale fits of Skyrme-type interactions to all available masses became feasible [25]. When including phenomenological correction terms for correlation effects, these Skyrme-force calculations compete with the best available microscopic-macroscopic models. Calculations with Gogny-type interaction are also on the way. More recent theoretical developments allow the large-scale microscopic calculation of correlation energies, either in the framework of a symmetry-restored Generator Coordinate Method [26], or a microscopic Bohr-Hamiltonian [27]. There is also a promising progress in Relativistic Mean Field models. We note that in addition to masses all these microscopic models aim to describe other nuclei properties such as, for example, nucleon densities. However, further development

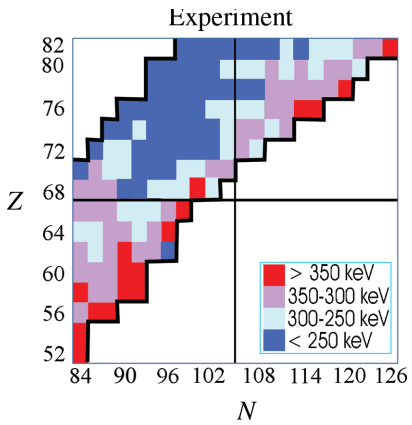

Figure 4. *δV_{pn} values in the rare-earth region in a Z-N chart, highlighting the symmetry of δV_{pn} with respect to shell closures and the need for data in the lower right quadrant.*

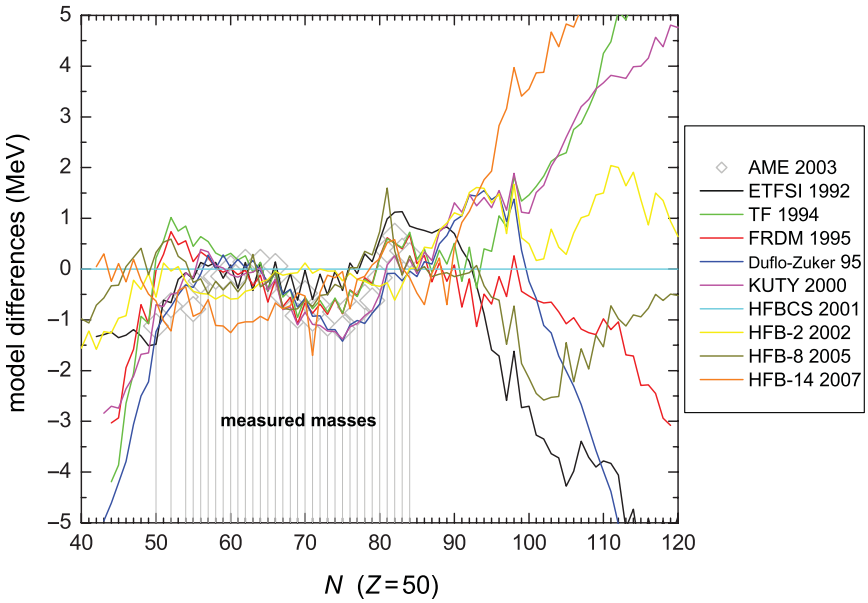

Figure 5. *Differences in mass predictions of various theoretical models and experimental data to predictions of the Hartree-Fock-Bogoliubov (HFBCS 2001) mass model as a function of N for tin isotopes (Sn, Z=50). Since the model parameters are adjusted to measured masses, the agreement is very good where masses are known [24].*

of the models is necessary to include all important correlation effects simultaneously, but the present results are most encouraging as they improve the predicted masses around shell closures. For a more reliable extrapolation of masses not only the models, but also the effective interactions used and the protocols for the adjustment of their coupling constants have to be improved. To that aim, it is highly desirable to collect further data on neutron-rich nuclei beyond the neutron shell closures that separate the stable nuclei from the drip line. Their structure is mainly determined by the single-particle states above the shell closures, which are not completely constrained by the data on more stable nuclei. Here, the new facilities under construction at, for example, FAIR, may deliver a large number of new data, either using a storage ring or the Penning trap technique.

Test of the Conserved Vector Current Hypothesis and the Unitarity of the CKM Matrix

The Cabibbo-Kobayashi-Maskawa (CKM) quark-mixing matrix V parameterizes the weak charged current interactions of quarks. Today the best possible direct test of its unitarity, which is a fundamental concept of the Standard Model, involves the top row of V, namely $|V_{ud}|^2+|V_{us}|^2+|V_{ub}|^2=1-\triangle$. In the Standard Model with a unitary CKM matrix, $\triangle$ is zero.

The most precise value for the V_{ud} element can be extracted from the vector coupling constant G_V derived from the mean Ft value of *superallowed nuclear β-decay*, in conjunction with the Fermi coupling constant from μ-decay G_μ: $V_{ud}{}^2 = G_V{}^2 / G_\mu{}^2$. Together with particle physics data from K and B meson decay, this can be used to test CKM unitarity. The experimental Ft value is expressed as:

$$Ft \equiv ft\,(1+\delta_R)(1-\delta_C) = K / (2|V_{ud}|^2\, G_\mu{}^2\,(1+\triangle_R)) = const.,$$

where δ_R is the nucleus-dependent radiative correction, δ_C the isospin-symmetry-breaking correction, and $\triangle_R$ the nucleus-independent radiative correction [29]. Experimentally, Ft is accessible by a combination of the decay energy Q, the half-life $T_{1/2}$, and the branching ratio R. The Q value enters to the fifth power into the calculation of the statistical rate function f and thus the masses of the mother and the daughter nuclei are needed with a precision of at least 1×10^{-8} in order to reach a relative uncertainty of the order of 0.1% on Ft. This is one of the most challenging applications of nuclear precision mass measurements, which can be addressed by Penning traps only. Here, concerning nuclear mass measurements, especially the Penning trap experiments at Argonne (CPT) [30], at ISOLDE (ISOLTRAP) [31], LEBIT [32], and IGISOL (JYFLTRAP) [33] have made significant contributions.

Recently improved calculations of the isospin-symmetry-breaking corrections addressed 20 superallowed β

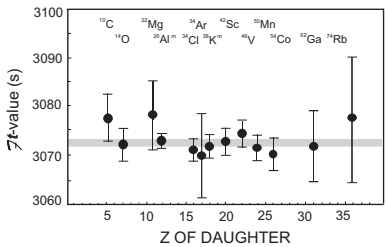

Figure 6. *Corrected experimental Ft-values for the 13 best-known super-allowed decays [28]. The grey band gives one standard deviation around the average Ft value.*

decays, which cover the nuclear chart from ^{10}C to ^{74}Rb [29]. A consistent picture for the 13 best-known cases confirmed the conserved-vector-current (CVC) hypothesis, which claims identical *Ft*-values for all transitions between isospin $T = 1$-analog states on the 10^{-4} level (Figure 4). With an averaged *Ft*-value of 3072.3(8) s, the up-down element of the CKM matrix results in $V_{ud} = 0.97402(26)$ and (using the V_{us} and V_{ub} values from the 2006 Particle Data Group review) yields $V_{ud}^2 + V_{us}^2 + V_{ub}^2 = 0.9997(10)$, that is, unitarity is satisfied with in an uncertainty of 0.1% [28].

Summary and Outlook

The masses of more than 1,000 short-lived radionuclides, that is, about one third of all known nuclides, have been directly determined by Penning trap and storage ring mass spectrometry. In many cases relative mass uncertainties down to 10^{-8} have been reached. The huge progress in measurement techniques is accompanied by recent developments in the ion-beam production of the exotic unstable nuclei. Further improvements can be expected from new research facilities with unprecedented rare-isotope production capabilities, such as, for example, SPIRAL2 at GANIL/Caen [34], FAIR at GSI/Darmstadt [35], Germany, RIBF at RIKEN/Wako [36] or a new advanced rare isotope accelerator in discussion in the United States [37]. Already the current measurements span the whole range from the lightest halo nuclei as, for example, ^{11}Li (recently measured with TITAN at TRIUMF [18]) to the superheavies like nobelium (which is in the focus of SHIPTRAP at GSI [38]). The new-generation facilities will produce nuclei further off the line of beta-stability, for example, many of the nuclides along the astrophysical r-process, where the mass values play an important role.

Acknowledgment

The authors express their gratitude to all colleagues within the field of high-precision mass spectrometry on short-lived nuclides, especially to R. Casten, J. C. Hardy, and D. Lunney for their valuable comments.

References

1. H.-J. Kluge, K. Blaum, and C. Scheidenberger, *Nucl. Instrum. Meth. A* 532, 48 (2004).
2. D. Lunney, J. M. Pearson, and C. Thibault, *Rev. Mod. Phys.* 75, 1021 (2003).
3. K. Blaum, *Phys. Rep*. 425, 1 (2006).
4. H. Geissel et al., *Ann. Rev. Nucl. and Part. Sci*. 45, 163 (1995).
5. U. Köster, *Eur. Phys. J.* A15, 255 (2002).
6. L. S. Brown and G. Gabrielse, *Rev. Mod. Phys*. 58, 233 (1986).
7. L. Schweikhard and G. Bollen (eds.), special issue *Int. J. Mass Spectrom*. 251 (2006).
8. B. Franzke, H. Geissel, and G. Münzenberg, *Mass Spectrom. Rev*., in press (2008).
9. B. Franzke, *Nucl. Instr. Meth. B* 24/25, 18 (1987).
10. H. Geissel et al., *Nucl. Instr. Meth. B* 70, 286 (1992).
11. F. Bosch et al., *Int. J. Mass Spectrom*. 251, 212 (2006).
12. Yu. A. Litvinov et al., *Nucl. Phys. A* 756, 3 (2005).
13. Yu. A. Litvinov et al., *Hyperfine Interactions* 173, 55 (2006).
14. M. Hausmann et al., *Nucl. Instr. Meth*. A446, 569 (2000).
15. F. Bosch, *J. Phys. B* 36, 585 (2003).
16. J. van Roosbroeck et al., *Phys. Rev. Lett*. 92, 112501 (2004).
17. M. Block et al., *Phys. Rev. Lett.* (2008).
18. J. Dilling et al., *Int. J. Mass Spectrom*. 251, 198 (2006).
19. B. Sun et al., *Eur. Phys, J.* A31, 393 (2007).
20. Yu. A. Litvinov et al., *Phys. Rev. Lett*. 95, 042501 (2005).
21. G. Audi, A. H. Wapstra, and C. Thibault, *Nucl. Phys. A* 729, 337 (2003).
22. R. B. Cakirli et al., *Phys. Rev. Lett*. 94, 092501 (2005).
23. Y. Oktem et al., *Phys. Rev. C* 74, 027304 (2006).
24. D. Lunney, private communication (2008).
25. S. Goriely et al., *Phys. Rev. C* 68, 054325 (2003).
26. M. Bender, G. F. Bertsch, and P.-H. Heenen, preprint nucl-th/0410023 (2004).
27. P. Fleischer et al., *Phys. Rev. C* 70, 054321 (2004).
28. J. C. Hardy, private communication (2008).
29. I. S. Towner and J. C. Hardy, *Phys. Rev. C* 77, 025501 (2008).
30. G. Savard et al., *Phys. Rev. Lett*. 95, 102501 (2005).
31. A. Kellerbauer et al., *Phys. Rev. Lett*. 93, 072502 (2004).
32. G. Bollen et al., *Phys. Rev. Lett*. 96, 152501 (2006).
33. T. Eronen et al., *Phys. Rev. Lett*. 100, 132502 (2008).
34. http://www.ganil.fr/research/developments/spiral2/
35. http://www.gsi.de/GSI-Future/CDR/
36. http://www.riken.go.jp/engn/r-world/research/lab/nishina/index.html
37. http://www.sc.doe.gov/np/program/FRIB.html
38. M. Block et al., *Eur. Phys. J. D* 45, 39 (2007).

KLAUS BLAUM
GSI Darmstadt, Darmstadt, Germany
Max-Planck-Institut für Kernphysik, Heidelberg, Germany

YURI A. LITVINOV
GSI Darmstadt, Darmstadt, Germany
Physikalisches Institut, Justus-Liebig-Universität Gießen, Gießen, Germany

LUTZ SCHWEIKHARD
Institut für Physik, Ernst-Moritz-Arndt-Universität Greifswald, Germany